9. Discussion, Conclusions and Outlook

9.1.1. Degree of localization

In Figure 9.1 we plot the number of active points (blue) against the westward drift curve of the South American plate, i.e., the upper plate (from Silver et al., 1998) for the last 46 Ma. This drift has an influence on the deformation mode of the upper plate (Heuret and Lallemand, 2005). For active points plotting below the velocity curve, the deformation distribution is localized, whereas it is rather diffuse when points plot above the curve. At 46 Ma, the velocity of westward drift is about 2 cm/year increasing to 3 cm/year during the evolution of the Central Andean plateau, showing that deformation was localized in the initial stage. Over time, more points became active within the plateau area and the Eastern Cordillera. Thus, two neighbouring structural units are active and deformation is distributed over a wider area, i.e., strain accumulates in a diffuse fashion. When deformation within the plateau becomes inactive after 10 Ma, strain accumulation "shifts" to the Subandean fold-and-thrust belt, where deformation again localizes.

9.1.2. Aspect ratios

Next, we plot aspect ratios of the geometry of the biggest active areas for a given Ma step in the same diagram (Fig. 9.1, green points). Aspect ratios can be calculated according to the characteristic widths and lengths of active areas. They yield values of 1 when the active areas have the same extent both orogen-parallel and orogen-normal. The value decreases the larger the length is compared to the width.

Again, we can see that strain initially accumulates at small structures of generally low aspect ratios. As soon as more points become active, the aspect ratio is 1, eventually decreasing again. This marks the time of first activity of neighbouring structural units, i.e., the plateau interior (the plateau and the Eastern Cordillera), with subsequent strain accumulation at the plateau margins. Further decrease of the aspect ratio shows increasing strain localization within narrow areas, namely the Subandean fold-and-thrust belt and parts of the Puna margin.

9.1.3. Frequency-size distribution

Figure 9.2 correlates the size of the actively deforming zones with their frequency of occurrence. The size is hereby defined as the number of neighbouring active points in our point grid for one area. Zones were grouped into classes covering five or ten points (e.g., 11 points, 16, 21, 26 points and so on). Zones with 60 points represent areas of e.g., 150 km width and 600 km length.

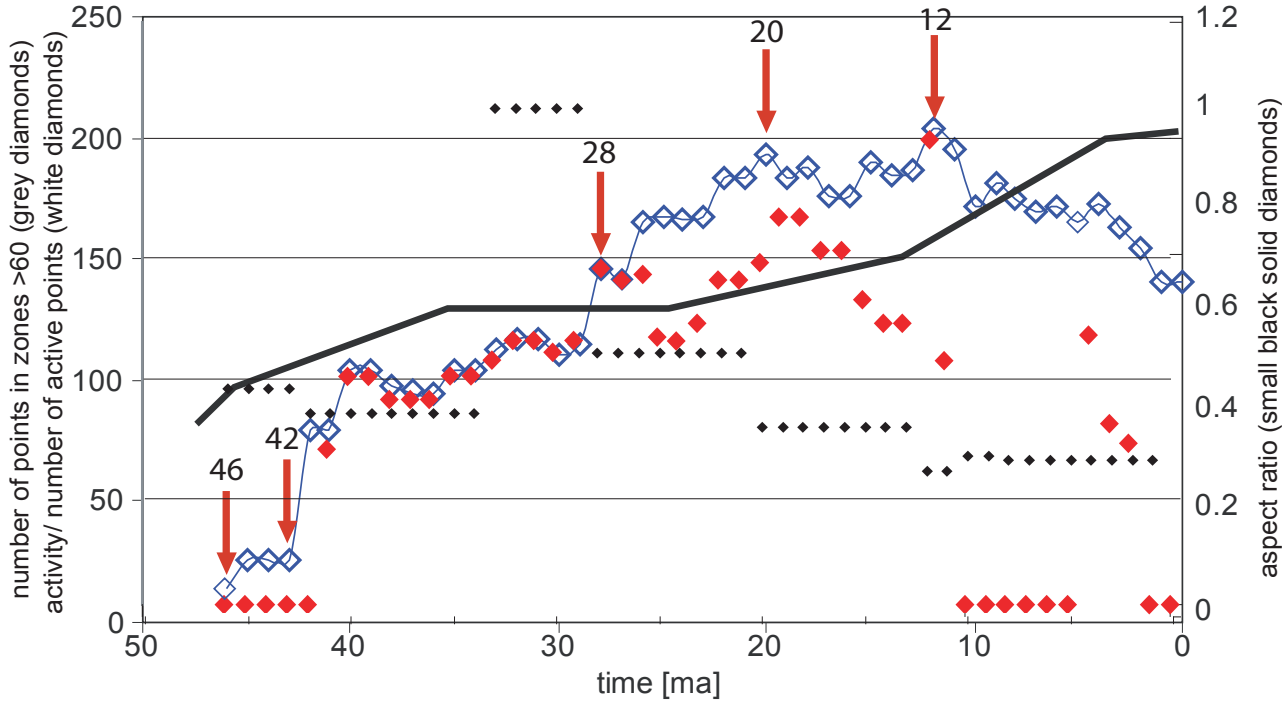

Fig. 9.1: Number of total active points per Ma (outlined diamonds), number of active points in areas with more than 60 neighbouring points (grey diamonds), aspect ratios (small black diamonds) and curve (black) of westward drift of South America (from Silver et al., 1998).

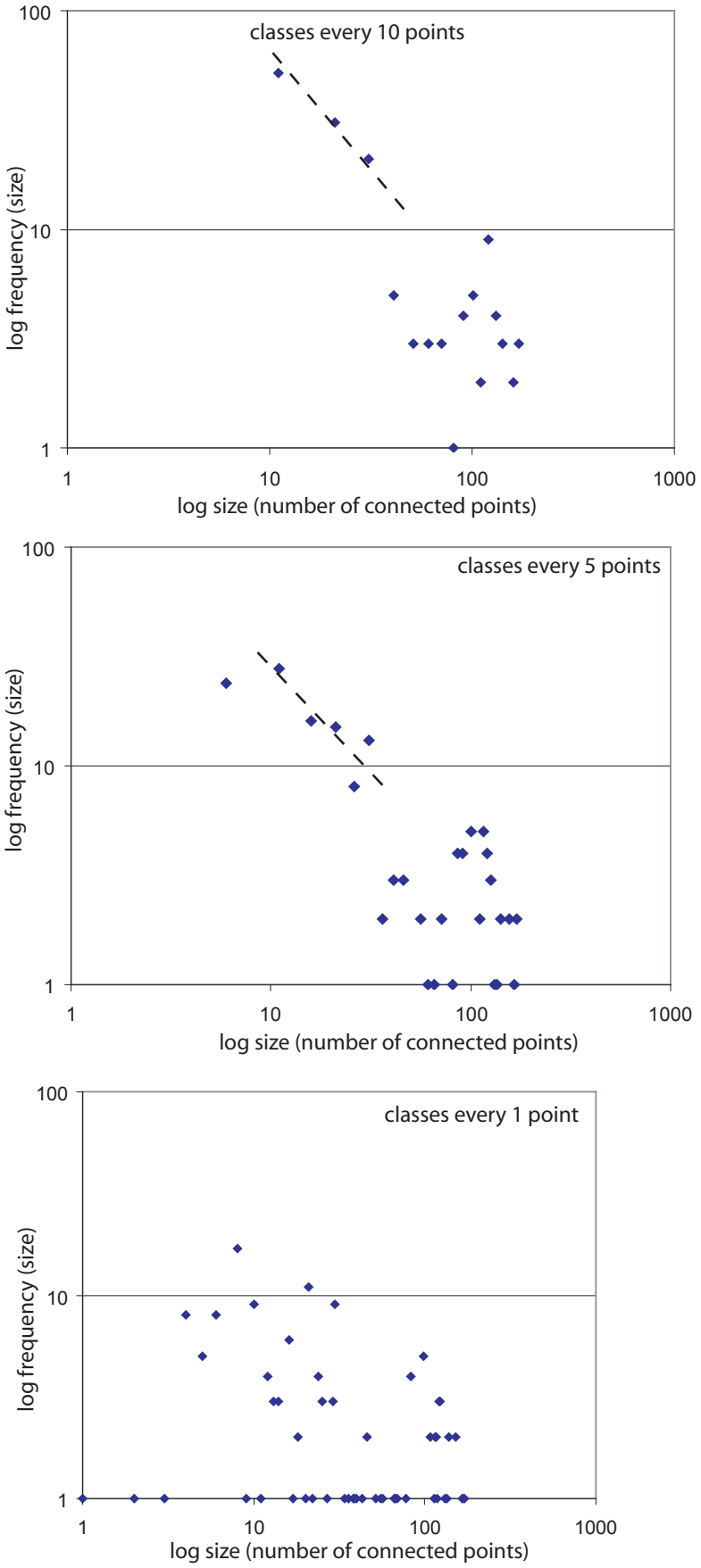

Fig. 9.2: Frequency-size distribution of active structures on the orogen scale in a log-log plot. The size of an active area is defined as the number of active neighbouring points. The three plots have different numbers of classes in which points are grouped. Cut-off values for classes are chosen below 11, 21, 31 points etc. for the figure at the top and every 6, 11, 16, 21 points etc. for the plot in the center. The plot at the bottom shows the original data without redistribution into classes. When classes are present, the points of small sizes could be approximated by a linear function (with a slope of ~ -1.8) up to a point beyond which points tend to cluster.

For areas with less than 60 points, the frequency size distribution indicates a power law over a very limited scale range for temporal sample windows of 1 Ma (dashed line with a slope of ~ -1.8, Fig. 9.2). Areas with more than 60 points are less frequent, and the power law ceases to be applicable. This cut-off value will shift towards smaller sizes (less points) when smaller time windows are sampled, due to better capability of resolving active structures of smaller extent. The cut-off value would move to the right for larger time windows, as we are summarizing several active structures. In this respect, for the finite pattern of the entire system over the total duration of deformation, every point will have been active at least once, representing an area with all points as active neighbours.

As proposed in Chapter 5, the active structures on the orogen scale are a multiple of the suborogen scale ones. This might be due to a summarizing effect of coevally active neighbours on the smaller scale. This summary is an unintentional integration of data in space to form a larger active area, which, when sampled with higher temporal and spatial resolution, will be divided into several small areas, as inactive areas may occur within originally large areas. So, the small areas in our frequency-size plot are real, whereas the areas with more than 60 points are not “real”, but only due to the summarizing effect arising from the resolution which is still too low.

9.1.4. Percentage of small vs. big areas

Based on the value of power law failure (Fig. 9.2), we calculated the number of active points that are part of areas with more than 60 points. The curve (Fig. 9.1, red points) shows that during the very first stage, when deformation was active only in a few regions in the Western and Eastern Cordillera (46-40 Ma), all points were active in areas with less than 60 points. Up to 27 Ma, almost all points were active in areas with more than 60 points, thus activity was clustered in large areas. From 26 to 11 Ma, the number of points varies, meaning that both large and small areas are active. From 10 Ma to the present, deformation became inactive in the plateau interior and shifted to the Subandean fold-and-thrust belt. Thus, another “initial” stage is represented by rather small areas. However, we have to bear in mind, that large areas are actually small areas: many coevally active and spatially neighbouring small areas.

9.1.5. Power spectra over time

When regarding the spatially distributed deformation values as signals, we can also examine them by means of auto-correlation, determining how well the data are correlated with themselves when shifted, e.g., in time. To analyze the variance of a signal over its frequency we apply a Fast Fourier Transform to generate energy spectra, or, in our case, power spectra. From the resulting power spectra (Fig. 9.3) we are now able to detect any underlying pattern in the variation of the variable for a given frequency (here spatial distance), e.g., patterns that are characteristic of deterministic or stationary stochastic processes (such as fractal patterns).

Figure 9.3 indicates that the power spectra of the shortening dataset in their current form reflect a fractal pattern of the spatial distribution of shortening rates per Ma from 36 Ma to 17 Ma. Generally, peaks in auto-correlation plots indicate characteristic lengths (Fig. 9.3). If these lengths of active deformation on the regional scales and their multiples on the orogen scale described in Chapter 5 were real, we should expect to find two peaks in the lag of the auto-correlation plots (x-axis). As we only observe one peak, the value is not periodical (i.e., not appearing for one length scale and again as a multiple for another length scale). Looking at the power spectra (Fig. 9.3), the only peak present for a lag of ~ -0.5 or 0.5 (e.g., for 40 Ma and 38 Ma) coincides with a bulge in the curve at about 100 km. This value is not equivalent to any value of the characteristic lengths described in Chapter 5. Rather, this alleged break in power law (indicated by the curve’s slope) is not a break in the scale-invariant distribution of shortening values, but an artefact of the balanced cross sections giving shortening estimates for one degree of latitude (~100 km). Therefore, in a N-S direction values show less variation for distances of ~100 km. This does however not preclude the general fractality over the scale range between 40 km (lower resolution cut-off) and 1000 km (upper resolution limit).

These plots will be subject of further examination with respect to their robustness against variation in the initial data set. Presently the shortening data follow the assumption that strain was homogeneously distributed in space and time (cf. 9.1.6. for discussion on properties of the dataset).

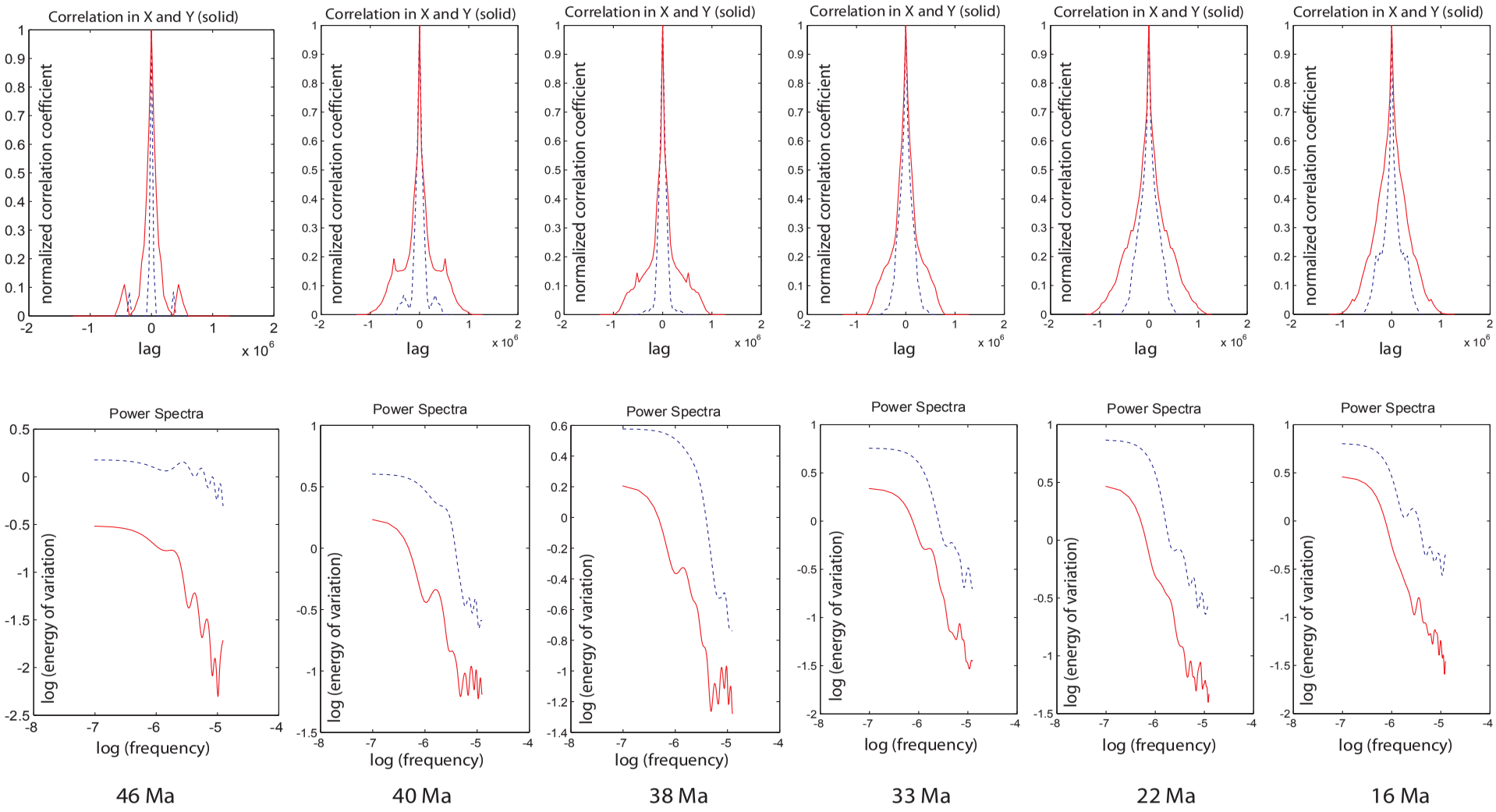

Fig. 9.3: Auto-correlation functions (top) and associated power spectra (bottom) for the spatial distribution of shortening rates per Ma (as given below each plot). The solid red curve depicts data in a N-S direction, and dashed blue data in E-W. More information in-text. Figures produced with Matlab codes by A. Levander.

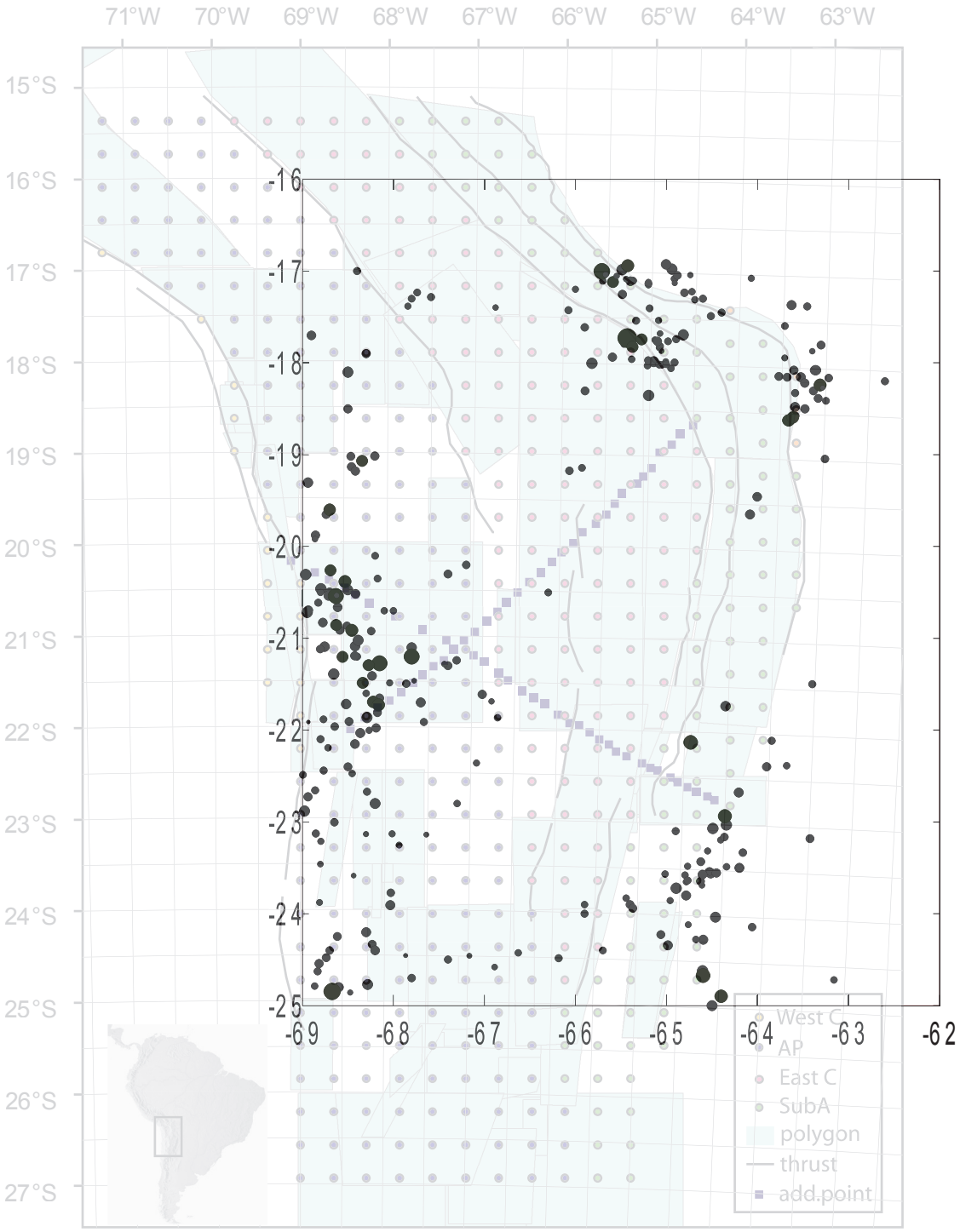

Fig. 9.4a: Distribution of earthquakes in the Central Andes. Earthquake data are from the NEIC catalogue including earthquakes that occurred between 1963-2006 up to a depth of 35 km and with magnitudes >3. The diameter is scaled to the destructed area at the surface (cf. Ritznitchenko, 1976).

9.1.6. Influence of quality of database

When compiling the data base we carefully paid attention to the quality of available deformation data, and included them only when the geographical position of their study areas and sample locations, the sample method for age dating, and the error of their measurements were precisely stated by the authors. Apart from the initial stages of deformation when only a few areas have been active, deformation data exist from more than one author for any studied area. When independent authors yield similar results, the data can be considered solid.

The study areas in the original data set generally have sizes of 100-200 km in length and width. Cases when authors have inferred a given deformation for a very big region up to ~600 km in length and ~300 km in width, are present only four

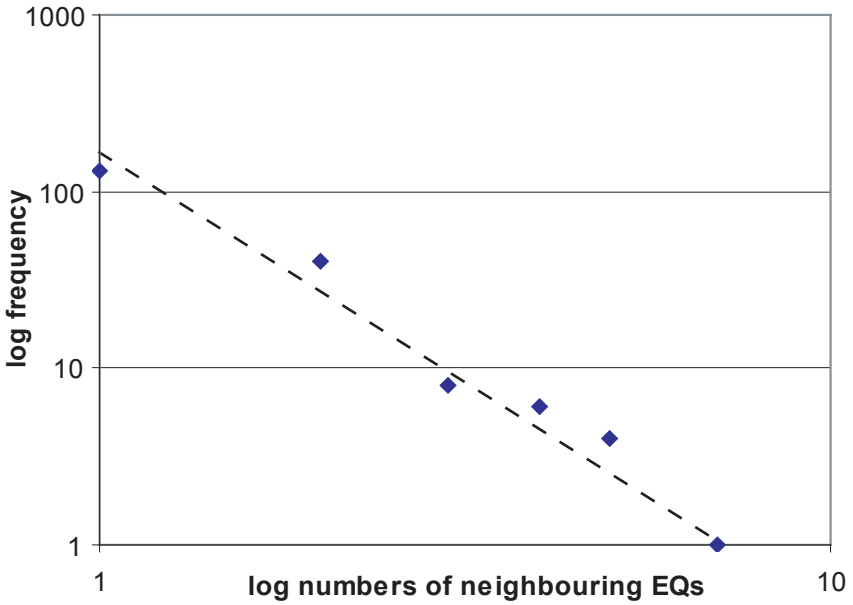

Fig. 9.4b: Frequency-size distribution of neighbouring earthquakes for the Central Andes (details in-text). Earthquakes are defined as neighbouring, when they share parts of their destructed surface area (cf. Fig. 9.4a).

times. As the characteristic length scales (with 150 km in width and 200-300 km in length), quantified in Chapter 5 neither have the same size as the small initial areas nor the large areas, the different study area sizes did not influence our results.

However, as we cannot resolve active structures below ~40-100 km, small areas are integrated into a large one simulating the above mentioned characteristic length scale. If our spatial resolution was better, we would be able to identify active and inactive parts within our regional areas, which would then break up into smaller areas. Thus, the characteristic length described in Chapter 5 must be seen as an artefact.

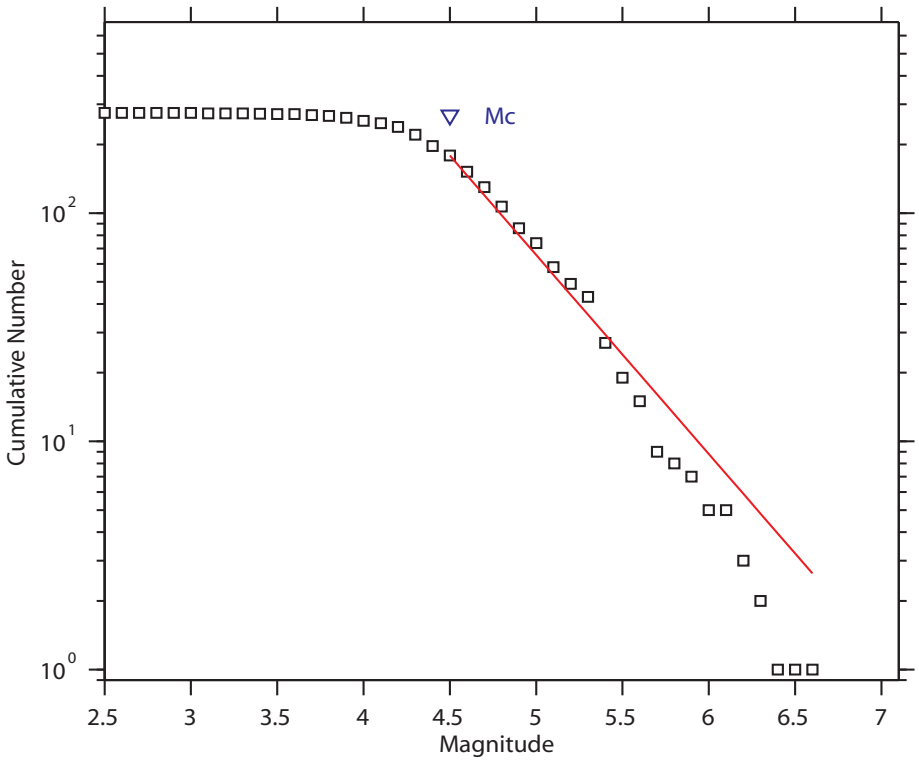

Maximum Likelihood Solution
b-value = 0.872 +/- 0.05, a value = 6.18, a value (annual) = 4.54
Magnitude of Completeness = 4.5

Fig. 9.4c: Magnitude-frequency distribution of earthquakes for the Central Andes (details in-text). Plotted with ZMap.

In contrast to the deformation activity data, which only have discrete values (0 or 1), the inferred shortening rates are more prone to inherit errors from the initial data set. To obtain a comprehensive data set with continuous rather than discrete values for such a large spatial extent down to a temporal resolution of only one million years, we had to accept the underlying assumption that both the spatial and temporal distribution of deformation was homogeneous. This affects the analysis of variation of values on scales $<10^2$ km for the E-W direction (i.e., we detect less variation $<10^2$ km), due to the fact that 1) the initial width of areas is 100 km or more, and 2) the structural units have extents of up to 300 km with known shortening estimates (e.g., the plateau or the Eastern Cordillera between 18 and 21°S). The N-S direction has a lack of variation for ~100 km (cf. 9.1.5.), as shortening estimates are very similar for each degree of latitude.

Some authors have worked with a higher spatial resolution (i.e., in smaller areas), but did not necessarily quantify the displacement for their study areas. In any case, the integration of a few higher resolved values among the majority of values with assumed homogeneity, would not change the correlation functions significantly. Despite being homogeneous, the correlation functions still change over time and for different analyzed directions (cf. Chapter 5 and Fig. 9.3). The next step is to evaluate the robustness of, e.g., correlation functions and power spectra against further changes and variation within the original data from the database. This can be done by comparing our results 1) to models of known underlying patterns, and 2) to a dataset that is less homogeneous than ours and one that is even more homogeneous. Future research should nevertheless attempt to increase the spatial resolution below 10^2 km, for example by consulting seismic sections for the quantification of both displacement and its timing.

9.2. Discussion

Power law relations of size-frequency distributions and spatial distributions of earthquakes and faults are commonly based on the respective finite patterns and therefore do not include the temporal evolution of a deformation system. But is the power law relation valid for all evolutionary stages of spatial distribution of deformation (earthquakes, faults and regional deformation) or only for the finite pattern?

Earthquakes follow the Gutenberg-Richter relation (e.g., Bak and Chang, 1989; Kagan and Jackson, 1991; Wesnousky, 1994) which correlates earthquake magnitudes with their frequency. This relation can only be established after a critical amount of earthquakes has occurred; in other words, when monitoring a completely undeformed domain from the beginning, it takes some time to accumulate several events before establishing a fractal pattern. Yet, this fractal pattern can only be observed when the sample time window is appropriately chosen: if the time window is too small, we would only sample single events (e.g., for an hour or a day); if it was too big, we would sample spatial clusters of deformation.

This clustering effect is also present when we assume that the spatial extent of earthquake occurrences is limited. In nature, any given spatial extent (i.e., study area of limited size) will be saturated at some time, with subsequent strain accumulation in another location.

We counted adjacent earthquakes (i.e, sharing a common destruction area, cf. Ritznitchenko, 1976) recorded between 1963 and 2006 for the Central Andean plateau (17°-25°S and 69°-63°W) in the upper plate down to 35 km depth with magnitudes >3 (Fig. 9.4a). Their zone size-frequency distribution (Fig. 9.4b) is similar to that of active areas (Fig. 9.2) insofar as they follow a power law distribution (slope ~ -2.4). Their magnitude-frequency relation has a power law with a b-value of ~0.87 (Fig. 9.4c).

The evolution of faults and fault systems in space is similar to that of earthquakes. In any completely undeformed domain, one or several faults develop first; more faults will occur with time, as earthquakes and aseismic events either increase the size of an existing fault, or lead to formation of a new fault. At some time, the spatial distribution of faults will establish a fractal pattern (e.g., Allègre et al., 1982; King, 1983; Turcotte, 1986) and their frequency-size distribution will follow a power law. Typical estimates for fractal dimensions are 1.7 (Sornette et al., 1990) or 1.8 (Marrett and Allmendinger, 1990) (cf. Bonnet et al., 2001 for a thorough review).

If we again consider a fixed spatial extent, there will be a time when the area is saturated with faults. Faults have eventually grown to their maximum possible lengths, and faulting will then move out of the area to form elsewhere, where

strain accumulation is more favourable. Thus, a once established fractal pattern will remain fractal in the future, as in the long run, strain accumulation occurs no longer in the first spatial extent (i.e., area in space) but a second rock volume where another fractal pattern will be established. Bonnet et al. (2001) point out that fault patterns are fractal due to the scale invariance of the fracture growth process arising from material heterogeneities in the crust.

The spatial size of such established fractal patterns will have the size of regional areas, e.g., ~150 km in width, 200-300 km in length or smaller (cf. Chapter 5), beyond which scale-invariance becomes invalid for sizes of active structures. As discussed before, this effect is due to the lack of spatial and temporal resolution beyond 40 km and 1 Ma, respectively. Thus, with the current resolution, large areas summarize smaller areas, which could otherwise be distinguished with higher resolution. In contrast, the shortening values are spatially distributed in a fractal way (cf. Section 9.1.5.). As mentioned before (9.1.6.), stability of results against variation in the initial data set has yet to be analyzed. However, in their present form, data reveal evolutionary stages of the spatial distribution and its fractal pattern in the Central Andes. Figure 9.1 shows that, in the beginning, only small areas are active (Western and Eastern Cordillera, 46-38 Ma), analogue to faults reaching a critical number before a fractal pattern can be established. These small regional areas will have established their fractal patterns by the end of this stage. In the next stage (37-16 Ma), the pattern will have evolved to be fractal also on the orogen scale (Fig. 9.3). At the “saturation stage”, the plateau no longer accumulates strain, and the pattern becomes stable. The establishment of the fractal pattern from the regional scale to the entire orogen can be comparably fast with ~8-10 Ma. Fractal fault patterns for a regional area of less than 100 km in the Puna has been similar or faster (Marrett and Allmendinger, 1990; Marrett et al., 1994).

At 10 Ma, the Subandean fold-and-thrust belt starts to deform, blurring the fractal pattern of the preceding stage, as we see now another initiation of strain accumulation in small areas which can already create a fractal pattern inside, as faults generally exhibit fractal patterns (e.g., references in Bonnet et al., 2001). The orogen itself is inactive and its distribution of active shortening is not fractal any more.

This procedure can be summarized: strain accumulation is initially diffuse or localized in “stage 1“ (depending on the dominant deformation mode, see below), balancing itself over a critical time period (or equivalent amount of strain) to become fractal for the regional area. By and by, a fractal pattern will also establish for the orogen, namely when several regional areas are active which themselves are fractal within (“stage 2”, fractal orogen). Once a fractal pattern is established for a given spatial extent (i.e., the analyzed area in space), strain accumulates in another “rock body” to repeat the procedure (initial “stage 3” with regional fractals). The first fractal pattern will be kept.

However, we can only observe these patterns, when the time window is well chosen to actually resolve the spatial extent of crucial features. For smaller structures (e.g., earthquakes or faults), the time window must be chosen relatively smaller, not to include structures that are part of another spatial extent or temporal stage. This effect is also relevant on the regional to orogen scale where we can only resolve time down to a million years (minimum). Therefore, active areas suggest a characteristic structural length on the regional scale, which will be a multiple on the orogen scale (cf. Chapter 5). In other words, the big scale merely summarizes the small scale as we might resolve structures of different temporal stages and spatial extents. This is due to the still too low temporal resolution and relatively big spatial sample extents precluding the identification of the underlying fractal pattern. This is also the reason why the power law is not valid beyond a value of 60 points (Fig. 9.2).

Ben-Zion and Sammis (2003) previously suggested that a finite fractal pattern exists, which balances strain hardening and weakening effects during its evolution. Thus, we also need to consider the differences between dominant processes and patterns, as the scaling relations might vary depending on what we analyze (also review by Bonnet et al., 2001). Deformation processes are effective on all spatial scales, and depending on the observed spatial and temporal scales, different deformation frameworks might be dominant (cf. Chapter 2). As we lack the high data resolution both in space and time, we do not know the various coupling relationships of processes and parameter effects within and across the scales (e.g., the influence of erosion on isostatic effects

and together on deformation).

Generally, some faults are dominantly active, losing their roughness with increased slip. This is a characteristic for the continuum-Euclidean deformation framework. Yet, this fault will not have a notable impact in a spatial distribution, and will simply be part of the frequency-size distribution as one of the long faults. This again shows that a fractal pattern does not determine which type of strain accumulation is dominant, e.g., strain hardening or strain weakening. Thus, the frameworks do not exclude each other, but they are coexisting or alternating in time and space (see summary by Ben-Zion and Sammis, 2003).

In general, the indicators for the continuum-Euclidean frameworks might be stronger as Regenauer-Lieb et al. (2006) pointed out. They have proposed a multi-scale approach with various weakening processes, effective on different spatial and temporal scales (i.e., grain size dependent creep processes in the time interval <1000 years; thermal diffusion processes within shear zones for hundred thousand years or more; and water weakening processes on millions of years and more).

Ben-Zion and Sammis (2003) also conclude that long-term evolution of deformation favours the first order influence of the continuum-Euclidean framework, due to its positive feedback mechanism associated with strain weakening. An explanation for this can again be found in the spatial resolution or the area size that is analyzed. As discussed above, we assumed an unlimited spatial extent, in which strain accumulation can eventually establish a fractal pattern. Heterogeneities in the crust produce zones of weakness, where strain preferably accumulates. This represents a limited spatial extent, as strain accumulation would rather accumulate in a weak zone than move outside, where strain localization is not favourable. Bonnet et al. (2001) state that the fracture growth process is scale-invariant due to material heterogeneities. With time, a weak zone will be saturated with strain, and eventually will not be a weak zone any more, as Townend and Zoback (2000) propose that faulting keeps the crust strong. Thus, at some evolutionary stage, a weak zone does not attract particular strain accumulation any longer, and a fractal pattern can generally be established.

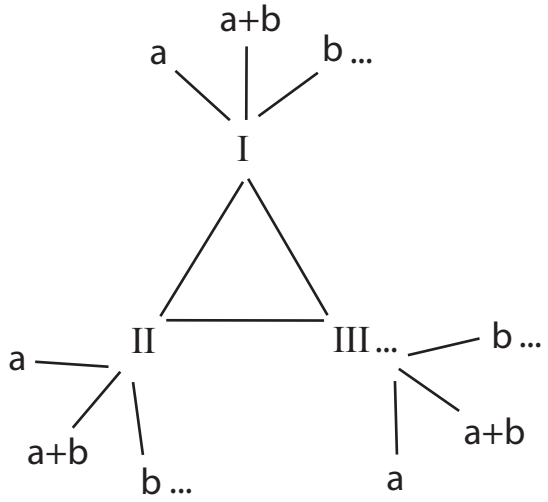

Fig. 9.5: Relation of causes and effects

More artificial reasons also suggest the continuum-Euclidean framework to be dominant over time: planar structures have been highly active (i.e., they have lost their initial roughness with increased slip), and their potential of being stored in the exposed rock record is much higher than for small structures that hardly accumulate strain. Also, faults cannot regain their roughness. Thus, a particular fault might be interpreted to be dominant at all times merely due to the lack of roughness, although it might not have had accumulated any strain over certain periods (and thus might have been part of a complex system in which all faults equally accumulate strain, or might have accumulated strain in a diffuse fashion).

The contribution of deformation processes to strain accumulation in space and time, which is in favour of different deformation frameworks, is further complicated by other processes that act on any deformation system. Causes and effects are not easily correlated (e.g., erosion and deformation), as these causes do not only become effective on one scale, but across the scales; and smaller scales “imprint” on the larger scales. This was shown in Chapter 7, where second order parameters have an effect on the regional scale (e.g., additional decoupling horizons), whereas the orogen scale pattern remains the same. In a schematic sketch (Fig. 9.5), it becomes clear that too many unknown variables exist, i.e., relations between causes and effects (a+I, b+I, a+b+I, a+II, b+II…, e.g., erosion and its effect on topography development and deformation), and between causes themselves (a+b, a+c…, e.g., climate and erosion) and effects themselves (I+II, II+III…, e.g., isostasy, topography and deformation). Yet, these relations might change over time. Thus, we might never fully understand highly complex coupled systems.

In Chapter 6, I studied the coupling relation between mechanical heterogeneities, namely basal (20%) and lateral (35%) strength contrasts for which threshold values exist that determine if either a plateau-style or a wedge-like system develops. I also showed that the relation between causes and effects does not produce a unique strain evolution in space and time. Thus, we cannot use the finite pattern for the relation of causes and effects, as it can be explained by more than one parameter combination.

The model results yield a similar spatiotemporal evolution to the one for the Central Andean plateau, yet with a very different parameter combination (for the latter coupling mechanical heterogeneities vs. differential trench-upper plate velocity evolution, high plate interface coupling from low trench infill, and the weak zones in the upper plate, cf. Oncken et al., 2006). In both experimental series, I was also able to show that there is a hierarchy among parameters affecting the system. Thus, some parameters (single or in combination) have first order influence actively changing the type of pattern (e.g., plate geometry, cf. Chapter 7). Second order effects can merely affect a pattern by varying the strain accumulation in space and time on a scale smaller than the entire system (e.g., additional decoupling horizons, cf. Chapter 7).

9.3. Conclusions

What did this study show?

1) Spatial distributions of deformation structures of all sizes (e.g., earthquakes, faults, and regionally active structures) have a fractal pattern and a power law relating size and frequency. However, depending on the available temporal and spatial resolution, the underlying patterns cannot always be identified, as 1. the resolution might not be appropriate for the analyzed structures (i.e., small structures need higher resolution to be detected), 2. too many structures might overlie each other for a given temporal sample length (i.e., if the time window is chosen too large, deformation events and structures might cluster), and 3. we unintentionally summarize structures on larger scales that belong to smaller ones, blurring the real pattern for the larger scale (cf. Chapter 5 and 9.1.6.).
2) Deformation systems undergo stages. The "initial" strain accumulation on the upper end of spatial scales (namely the orogen scale and the next smaller regional scale) is limited to a few active regional areas with a fractal fault pattern (cf., e.g., Bonnet et al., 2001). On these lines, the initial strain accumulation in the Western and Eastern Cordillera from 46 Ma to ~38 Ma commonly occurs in such structures that are 150 km in width (E-W) and 200-300 km in length (N-S) for the used spatial and temporal resolution, and have established a fractal pattern at the end of this stage.
3) Over time, more regional areas with a fractal pattern become active throughout the entire orogen. Therefore, the spatial distribution of shortening follows a power law for the entire orogen during a second stage of Central Andean plateau formation, i.e., from ~37 Ma to ~16 Ma.
4) Once a spatial extent or "rock volume" is saturated with strain, strain will accumulate elsewhere. The above mentioned stages can therefore repeat themselves in another area. This occurs after 15 Ma, when the plateau interior becomes stable and strain accumulation will occur in the Interandean and eventually in the Subandean (after 10 Ma). The fractal pattern of the first established stage is preserved.
5) A fractal pattern can result irrespectively of the various deformation processes that coexist or alternate during strain evolution (e.g., strain hardening and weakening). However, effects of the different deformation processes as well as other factors influencing a deformation system, can blur the underlying patterns and preclude their identification.
6) Various controlling factors have either a first order impact on a deformation system, thereby actively changing the orogen scale pattern (e.g., plate geometry, cf. Chapter 7), or a second order influence, thus affecting only the suborogen scales (e.g., additional decoupling horizons).
7) Parameters themselves are likely to be coupled and therefore have a different influence on a deformation system than if they acted alone. Threshold values exist that determine either one or another type of

e.g., deformation mode or the resulting type of deformation system. This was shown in Chapter 6, where threshold values for basal (20%) and lateral strength contrasts (35%) coupled together, determine the result to be wedge-like or plateau-style. There are no gradual transitions in between these two types.

8) The spatiotemporal evolution of the Central Andean plateau was reproduced on the orogen scale and below in analogue models that followed a parameter combination of mechanical heterogeneities. In contrast, the parameter combination in nature is supposed to be more complex. This shows that a strain pattern can be caused by more than one parameter combination and is therefore not unique. Thus, we cannot conclude the controlling parameters from the observed strain patterns.

9.4. Future research

First of all we should always bear in mind that scaling up and down of processes or patterns is only valid, when they follow a similar mathematical relation. However, even if the pattern or process is generally scale-invariant, it might look different on some scales thereby suggesting scale-dependent behaviour, depending on the temporal and spatial resolution, the current deformation mode within a structure of a deformation system, and the evolutionary stage of the system.

Therefore, we should aim for an even more comprehensive database including deformation data with a higher spatial resolution, allowing areas and variation of strain accumulation to be resolved below 40 km. This can probably be done with the help of seismic sections covering a 3D volume, where information on the displacement of faults and their timing is gained from the stratigraphy. This would certainly require a lot of seismic sections. Possibly, for the later stages of deformation, paleoseismological data could be integrated when available in order to also increase the temporal resolution. Again, the robustness of data results against uncertainty in the initial data set has to be examined.

Also, we need to mathematically quantify geological observations and changes over time on different spatial scales. Unfortunately, outcrops where a given spatial pattern can be studied over various time scales are very rare. And it is almost impossible to relate processes and patterns over time from outcrop data.

Certainly, our best resolved data are still those from modelling studies. They should try to quantify existing threshold values, and the robustness of studied parameters, e.g., by coupling them to other parameters (Is it still the same effect or not? Does the parameter have a first or second order influence?). The knowledge of threshold values simplifies the understanding of a particular parameter influence.

If modelling studies directly address a certain natural example (rather than staying general to be applicable to several similar natural examples), we can better relate the modelling study to natural data on smaller scales as well. Generally, models reproduce the big scale strain patterns for different orogens, which might look alike. However, as was shown in the viscous-brittle series (Chapter 7), even though a strain pattern on the orogen-scale looks similar, the variation on the subscales might be significantly different. Further modelling on the smaller scales should involve detailed analysis of small scale processes such as, e.g., fluid flow and fluid reactions.